Available online at www.sciencedirect.com
SCIENCE DIRECT®
Surface Science 554 (2004) 245–252
SURFACE SCIENCE
www.elsevier.com/locate/susc

An alternative way of calculating the superlattice Green function for discrete media

S.J. Vlaev [a,*], I. Rodríguez-Vargas [b], L.M. Gaggero-Sager [b], V.R. Velasco [c]

[a] Escuela de Física, Universidad Autónoma de Zacatecas, Apartado postal C-580 Zacatecas, Zac., Mexico
[b] Facultad de Ciencias, Universidad Autónoma del Estado de Morelos, Av. Universidad 1001, CP. 62210 Cuernavaca, MOR., Mexico
[c] Instituto de Ciencia de Materiales de Madrid, CSIC, Cantoblanco, 28049 Madrid, Spain

Received 20 November 2003; accepted for publication 3 February 2004

Abstract

We present an alternative and efficient way for calculating the superlattice Green function for discrete systems. The idea is to consider the superlattices as a crystal with the unit cell having the size of the superlattice period in the growth direction. The calculation method takes into account the matrix structure of the system Hamiltonian and a block tridiagonal matrix inversion algorithm. To illustrate the method we study the electronic band structure of a semiconductor superlattice described by means of an empirical sp^3s^* tight-binding Hamiltonian, including nearest-neighbor interactions and spin–orbit coupling.

Keywords: Superlattices; Green's function methods; Surface electronic phenomena (work function, surface potential, surface states, etc.)

1. Introduction

The most common types of heterostructures are simple heterojunctions, quantum wells and superlattices [1,2]. These multilayer structures are produced now with a high quality degree due to the enormous advances in growth techniques such as molecular beam epitaxy (MBE) and metal-organic chemical vapour deposition (MOCVD). In particular GaAs/AlAs superlattices received considerable attention as prototypes of artificial heterostructures combining alternate slabs of a direct-gap material (GaAs) and an indirect-gap one (AlAs), which resulted in novel electronic features such as band mixing or spatial confinement. The control now achieved in the growth of heterostructures has made possible the existence of more complicated heterostructures of interest. As examples we can quote an arbitrary sequence of wells and barriers, digital quantum wells [3], polytype superlattices [4] or a quasiregular system following a given sequence (Fibonacci, Thue-Morse, etc.) [5,6]. The usual superlattices have a great importance in different fields, but especially in the laser device area. Quantum cascade lasers

* Corresponding author.
E-mail address: stoyanv@cantera.reduaz.mx (S.J. Vlaev).

0039-6028/$ - see front matter © 2004 Published by Elsevier B.V.
doi:10.1016/j.susc.2004.02.007

based on the intraband transitions of GaAs/AlAs superlattices [7] have been produced. One of the advantages of superlattices in laser design comes from the high oscillator-strength of the radiative transitions between minibands. This leads to the so called "natural inversion", and in contrast to the case of the intersubband quantum cascade structures, comes for free.

Different theoretical methods have been put forward to study these systems. Recent review works on the theoretical methods employed to study multilayer and nanostructured systems can be found in [8,9]. Among these methods, Green's function techniques have proved to be very useful for these studies. Among the Green's function techniques the surface Green's function matching (SGFM) [10–12] and the interface response theory [13,14] are very handy to study systems with many non-equivalent interfaces because they are particularly compact and flexible. These methods obtain the system Green function through the bulk Green functions of the constituent materials. We present here an alternative and efficient way to calculate the Green function of a superlattice (simple or polytype) in discrete media by considering the whole superlattice period.

In Section 2 we present the mathematical method. In Section 3 an application is done to the study of the electronic structure of GaAs/AlAs superlattices described by an empirical tight-binding (ETB) sp^3s^* Hamiltonian [15] including nearest-neighbor interactions and spin–orbit coupling [16]. Conclusions are presented in Section 4.

2. Mathematical method

We shall consider an infinite superlattice A_{n_w}/B_{n_b}, with n_w monolayers of material A and n_b monolayers of material B, described as discrete media. The problem to study can be electronic states, phonons, etc., with no loss of generality in our method. The main idea of the method is to consider the superlattice as a crystal, although artificial, having as unit cell the superlattice period in the growth direction, taken here as the z axis. Then we proceed with a generalization of the classical method for surfaces and interfaces [17] to the superlattice case.

In order to fix the notation we shall take the wording of the electronic structure problem, but the method is not restricted to this problem, and it is easy to see how it can be applied to the study of other excitations in superlattices.

We shall consider an infinite SL having n_w monolayers of well material (A) and n_b monolayers of barrier material (B) in each SL period $d = n_w + n_b$. We can generalize now the concept of principal layer [18] to the SL period d. The principal layer indices are in this case $N-1$, N, $N+1$. The layer Hamiltonian (dynamical matrix, etc.) takes the form

$$\mathbf{H}_{N,N} = \begin{bmatrix} \mathbf{H}_{w_N,w_N} & \mathbf{H}_{w_N,b_N} \\ \mathbf{H}_{b_N,w_N} & \mathbf{H}_{b_N,b_N} \end{bmatrix} \tag{1}$$

$$\mathbf{H}_{N,N+1} = \begin{bmatrix} 0 & 0 \\ \mathbf{H}_{b_N,w_{N+1}} & 0 \end{bmatrix} \tag{2}$$

$$\mathbf{H}_{N,N-1} = \begin{bmatrix} 0 & \mathbf{H}_{w_N,b_{N-1}} \\ 0 & 0 \end{bmatrix} \tag{3}$$

"b" and "w" stand here for barrier and well respectively. The Hamiltonian elements $\mathbf{H}_{N,N}$, $\mathbf{H}_{N,N+1}$ and $\mathbf{H}_{N,N-1}$ are $((n_b+n_w)M \times (n_b+n_w)M)$ supermatrices, M being the size of the Hamiltonian element imposed by the model we are using. $\mathbf{H}_{w,w}$, $\mathbf{H}_{w,b}$, $\mathbf{H}_{b,w}$, $\mathbf{H}_{b,b}$ are supermatrices too. Because in general n_w will be different from n_b, $\mathbf{H}_{w,b}$, $\mathbf{H}_{b,w}$ are rectangular supermatrices, while $\mathbf{H}_{w,w}$ and $\mathbf{H}_{b,b}$ are square supermatrices. As we told before the size of M depends on the model we are using. If we use a sp^3s^* ETB Hamiltonian with nearest-neighbor interactions and spin–orbit coupling for zinc-blende semiconductors, then $M = 20$. The $\mathbf{H}_{N,N}$ matrix is a block tridiagonal one, whereas $\mathbf{H}_{N,N+1}$ and $\mathbf{H}_{N,N-1}$ have only a non-zero block. These matrices have the following structure

$$\mathbf{H}_{N,N} = \begin{bmatrix} \mathbf{H}_{1,1} & \mathbf{H}_{1,2} & 0 & \cdots & \cdots & & 0 \\ \mathbf{H}_{2,1} & \mathbf{H}_{2,2} & \mathbf{H}_{\mathbf{2,3}} & 0 & \cdots & & \vdots \\ 0 & \mathbf{H}_{\mathbf{3,2}} & \ddots & \ddots & & 0 & \vdots \\ \vdots & 0 & \ddots & \ddots & \ddots & & 0 \\ \vdots & \vdots & 0 & \ddots & \mathbf{H}_{n_w+n_b-1,n_w+n_b-1} & \mathbf{H}_{n_w+n_b-1,n_w+n_b} & \\ 0 & \cdots & \cdots & 0 & \mathbf{H}_{n_w+n_b,n_w+n_b-1} & \mathbf{H}_{n_w+n_b,n_w+n_b} & \end{bmatrix} \tag{4}$$

$$\mathbf{H}_{N,N+1} = \begin{bmatrix} 0 & 0 & 0 & \cdots & \cdots & 0 \\ 0 & 0 & 0 & 0 & \cdots & \vdots \\ 0 & 0 & \ddots & \ddots & \vdots & \vdots \\ \vdots & 0 & \ddots & \ddots & \ddots & 0 \\ 0 & 0 & \vdots & \ddots & 0 & 0 \\ \mathbf{H}_{n_w+n_b,1} & 0 & \cdots & 0 & 0 & 0 \end{bmatrix} \tag{5}$$

$$\mathbf{H}_{N,N-1} = \begin{bmatrix} 0 & 0 & 0 & \cdots & 0 & \mathbf{H}_{1,n_w+n_b} \\ 0 & 0 & 0 & 0 & \cdots & 0 \\ 0 & 0 & \ddots & \ddots & 0 & \vdots \\ \vdots & 0 & \ddots & \ddots & \ddots & 0 \\ \vdots & \vdots & \vdots & \ddots & 0 & 0 \\ 0 & \cdots & \cdots & 0 & 0 & 0 \end{bmatrix} \tag{6}$$

In order to simplify the algorithm to calculate the Green function we shall define

$$\begin{aligned} \mathbf{W}_0^{\mathrm{SL}} &= E\mathbf{1} - \mathbf{H}_{N,N} \\ \boldsymbol{\alpha}_0^{\mathrm{SL}} &= \mathbf{H}_{N,N+1} \\ \boldsymbol{\beta}_0^{\mathrm{SL}} &= \mathbf{H}_{N,N-1} \end{aligned} \tag{7}$$

where in fact E is to be understood, as usual, as the limit of $E + \mathrm{i}\epsilon$ for $\epsilon \to 0$.

The Green's function equation is given by

$$(E\mathbf{1} - \mathbf{H}) \cdot \mathbf{G} = \mathbf{1} \tag{8}$$

or in an equivalent form

$$\begin{aligned} &-\mathbf{H}_{N,N-1} \cdot \mathbf{G}_{N-1,M} + (E\mathbf{1} - \mathbf{H})_{N,N} \cdot \mathbf{G}_{N,M} \\ &\quad - \mathbf{H}_{N,N+1} \cdot \mathbf{G}_{N+1,M} = \boldsymbol{\delta}_{N,M} \end{aligned} \tag{9}$$

This expression is really an infinite system of equations. By taking into account the layer structure of the Hamiltonians involved the former equation can be written as

$$\begin{aligned} &\vdots \\ &-\boldsymbol{\alpha}_0^{\mathrm{SL}} \cdot \mathbf{G}_{-3,0} + \mathbf{W}_0^{\mathrm{SL}} \cdot \mathbf{G}_{-2,0} - \boldsymbol{\beta}_0^{\mathrm{SL}} \cdot \mathbf{G}_{-1,0} = \mathbf{0} \\ &-\boldsymbol{\alpha}_0^{\mathrm{SL}} \cdot \mathbf{G}_{-2,0} + \mathbf{W}_0^{\mathrm{SL}} \cdot \mathbf{G}_{-1,0} - \boldsymbol{\beta}_0^{\mathrm{SL}} \cdot \mathbf{G}_{0,0} = \mathbf{0} \\ &-\boldsymbol{\alpha}_0^{\mathrm{SL}} \cdot \mathbf{G}_{-1,0} + \mathbf{W}_0^{\mathrm{SL}} \cdot \mathbf{G}_{0,0} - \boldsymbol{\beta}_0^{\mathrm{SL}} \cdot \mathbf{G}_{1,0} = \mathbf{1} \\ &-\boldsymbol{\alpha}_0^{\mathrm{SL}} \cdot \mathbf{G}_{0,0} + \mathbf{W}_0^{\mathrm{SL}} \cdot \mathbf{G}_{1,0} - \boldsymbol{\beta}_0^{\mathrm{SL}} \cdot \mathbf{G}_{2,0} = \mathbf{0} \\ &-\boldsymbol{\alpha}_0^{\mathrm{SL}} \cdot \mathbf{G}_{1,0} + \mathbf{W}_0^{\mathrm{SL}} \cdot \mathbf{G}_{2,0} - \boldsymbol{\beta}_0^{\mathrm{SL}} \cdot \mathbf{G}_{3,0} = \mathbf{0} \\ &\vdots \end{aligned} \tag{10}$$

We can eliminate from these equations all the odd-numbered layers, by formally solving for $\mathbf{G}_{2n\pm1,0}$. In this way we obtain a new system of equations

$$\begin{aligned} &\vdots \\ &-\bar{\boldsymbol{\alpha}}_0^{\mathrm{SL}} \cdot \mathbf{G}_{-6,0} + \overline{\mathbf{W}}_0^{\mathrm{SL}} \cdot \mathbf{G}_{-4,0} - \bar{\boldsymbol{\beta}}_0^{\mathrm{SL}} \cdot \mathbf{G}_{-2,0} = \mathbf{0} \\ &-\bar{\boldsymbol{\alpha}}_0^{\mathrm{SL}} \cdot \mathbf{G}_{-4,0} + \overline{\mathbf{W}}_0^{\mathrm{SL}} \cdot \mathbf{G}_{-2,0} - \bar{\boldsymbol{\beta}}_0^{\mathrm{SL}} \cdot \mathbf{G}_{0,0} = \mathbf{0} \\ &-\bar{\boldsymbol{\alpha}}_0^{\mathrm{SL}} \cdot \mathbf{G}_{-2,0} + \overline{\mathbf{W}}_0^{\mathrm{SL}} \cdot \mathbf{G}_{0,0} - \bar{\boldsymbol{\beta}}_0^{\mathrm{SL}} \cdot \mathbf{G}_{2,0} = \mathbf{1} \\ &-\bar{\boldsymbol{\alpha}}_0^{\mathrm{SL}} \cdot \mathbf{G}_{0,0} + \overline{\mathbf{W}}_0^{\mathrm{SL}} \cdot \mathbf{G}_{2,0} - \bar{\boldsymbol{\beta}}_0^{\mathrm{SL}} \cdot \mathbf{G}_{4,0} = \mathbf{0} \\ &-\bar{\boldsymbol{\alpha}}_0^{\mathrm{SL}} \cdot \mathbf{G}_{2,0} + \overline{\mathbf{W}}_0^{\mathrm{SL}} \cdot \mathbf{G}_{4,0} - \bar{\boldsymbol{\beta}}_0^{\mathrm{SL}} \cdot \mathbf{G}_{6,0} = \mathbf{0} \\ &\vdots \end{aligned} \tag{11}$$

where

$$\overline{\mathbf{W}}_0^{\mathrm{SL}} = \mathbf{W}_0^{\mathrm{SL}} - \boldsymbol{\beta}_0^{\mathrm{SL}} (\mathbf{W}_0^{\mathrm{SL}})^{-1} \boldsymbol{\alpha}_0^{\mathrm{SL}} - \boldsymbol{\alpha}_0^{\mathrm{SL}} (\mathbf{W}_0^{\mathrm{SL}})^{-1} \boldsymbol{\beta}_0^{\mathrm{SL}} \tag{12}$$

$$\bar{\boldsymbol{\beta}}_0^{\mathrm{SL}} = \boldsymbol{\beta}_0^{\mathrm{SL}} (\mathbf{W}_0^{\mathrm{SL}})^{-1} \boldsymbol{\beta}_0^{\mathrm{SL}} \tag{13}$$

$$\bar{\boldsymbol{\alpha}}_0^{\mathrm{SL}} = \boldsymbol{\alpha}_0^{\mathrm{SL}} (\mathbf{W}_0^{\mathrm{SL}})^{-1} \boldsymbol{\alpha}_0^{\mathrm{SL}} \tag{14}$$

In this way we have obtained similar equations to (10) with renormalized matrices. This procedure can now be iterated, and at any step, say i, we obtain the following matrices as a function of those obtained in step $i-1$

$$\mathbf{W}_i^{\mathrm{SL}} = \mathbf{W}_{i-1}^{\mathrm{SL}} - \boldsymbol{\beta}_{i-1}^{\mathrm{SL}} (\mathbf{W}_{i-1}^{\mathrm{SL}})^{-1} \boldsymbol{\alpha}_{i-1}^{\mathrm{SL}} - \boldsymbol{\alpha}_{i-1}^{\mathrm{SL}} (\mathbf{W}_{i-1}^{\mathrm{SL}})^{-1} \boldsymbol{\beta}_{i-1}^{\mathrm{SL}} \tag{15}$$

$$\boldsymbol{\beta}_i^{\mathrm{SL}} = \boldsymbol{\beta}_{i-1}^{\mathrm{SL}} (\mathbf{W}_{i-1}^{\mathrm{SL}})^{-1} \boldsymbol{\beta}_{i-1}^{\mathrm{SL}} \tag{16}$$

$$\boldsymbol{\alpha}_i^{\mathrm{SL}} = \boldsymbol{\alpha}_{i-1}^{\mathrm{SL}} (\mathbf{W}_{i-1}^{\mathrm{SL}})^{-1} \boldsymbol{\alpha}_{i-1}^{\mathrm{SL}} \tag{17}$$

From here we can apply the same formal procedure used for a homogeneous bulk medium [17]. As opposed to the structural Green function [11,19] we do not need the $1D$ wavevector $\mathbf{k}_{\mathrm{SL}}$ associated to the superperiodicity of the structure. In this way we eliminate the need to integrate over $\mathbf{k}_{\mathrm{SL}}$ in order to obtain the normal superlattice Green function. The price to pay for this fact is an increase in the size of the matrices entering the algorithm, especially if n_{w} and n_{b} are large numbers. We shall see that this can be overcome with relative ease due to the structure of the different supermatrices involved. It has been noted before that $\mathbf{H}_{N,N}$ is always block tridiagonal while $\mathbf{H}_{N,N-1}$, $\mathbf{H}_{N,N+1}$ have only one non-zero block.

It is then clear that the matrices entering the iteration procedure are given by

$$\mathbf{W}_0^{\mathrm{SL}} = \begin{bmatrix} \mathbf{w}_0^{\mathrm{w}} & \boldsymbol{\alpha}_0^{\mathrm{w}} & 0 & \cdots & \cdots & 0 \\ \boldsymbol{\beta}_0^{\mathrm{w}} & \mathbf{w}_0^{\mathrm{w}} & \boldsymbol{\alpha}_0^{\mathrm{w}} & 0 & \cdots & \vdots \\ 0 & \boldsymbol{\beta}_0^{\mathrm{w}} & \ddots & \ddots & 0 & \vdots \\ \vdots & 0 & \ddots & \ddots & \ddots & 0 \\ \vdots & \vdots & 0 & \ddots & \mathbf{w}_0^{\mathrm{b}} & \boldsymbol{\alpha}_0^{\mathrm{b}} \\ 0 & \cdots & \cdots & 0 & \boldsymbol{\beta}_0^{\mathrm{b}} & \mathbf{w}_0^{\mathrm{b}} \end{bmatrix} \tag{18}$$

$$\boldsymbol{\alpha}_0^{\mathrm{SL}} = \begin{bmatrix} 0 & 0 & 0 & \cdots & \cdots & 0 \\ 0 & 0 & 0 & 0 & \cdots & \vdots \\ 0 & 0 & \ddots & \ddots & \ddots & \vdots \\ \vdots & 0 & \ddots & \ddots & \ddots & 0 \\ 0 & 0 & \vdots & \ddots & 0 & 0 \\ \boldsymbol{\alpha}_0^{\mathrm{bw}} & 0 & \cdots & 0 & 0 & 0 \end{bmatrix} \tag{19}$$

$$\boldsymbol{\beta}_0^{\mathrm{SL}} = \begin{bmatrix} 0 & 0 & 0 & \cdots & 0 & \boldsymbol{\beta}_0^{\mathrm{wb}} \\ 0 & 0 & 0 & 0 & \cdots & 0 \\ 0 & 0 & \ddots & \ddots & \ddots & \vdots \\ \vdots & 0 & \ddots & \ddots & \ddots & 0 \\ \vdots & \vdots & \ddots & \ddots & 0 & 0 \\ 0 & \cdots & \cdots & 0 & 0 & 0 \end{bmatrix} \tag{20}$$

In the case of the first iteration we have

$$\mathbf{W}_1^{\mathrm{SL}} = \mathbf{W}_0^{\mathrm{SL}} - \boldsymbol{\beta}_0^{\mathrm{SL}} (\mathbf{W}_0^{\mathrm{SL}})^{-1} \boldsymbol{\alpha}_0^{\mathrm{SL}} - \boldsymbol{\alpha}_0^{\mathrm{SL}} (\mathbf{W}_0^{\mathrm{SL}})^{-1} \boldsymbol{\beta}_0^{\mathrm{SL}} \tag{21}$$

$$\boldsymbol{\beta}_1^{\mathrm{SL}} = \boldsymbol{\beta}_0^{\mathrm{SL}} (\mathbf{W}_0^{\mathrm{SL}})^{-1} \boldsymbol{\beta}_0^{\mathrm{SL}} \tag{22}$$

$$\boldsymbol{\alpha}_1^{\mathrm{SL}} = \boldsymbol{\alpha}_0^{\mathrm{SL}} (\mathbf{W}_0^{\mathrm{SL}})^{-1} \boldsymbol{\alpha}_0^{\mathrm{SL}} \tag{23}$$

The time consuming step here is the inversion of the block tridiagonal $\mathbf{W}_0^{\mathrm{SL}}$ matrix, but we shall see that the structure of the matrices entering the iteration procedure allows for a great simplification. The matrix $(\mathbf{W}_0^{\mathrm{SL}})^{-1}$ has all its elements non-zero. On the other hand $\boldsymbol{\alpha}_0^{\mathrm{SL}}$ given by (19) has only the lowest left element non-zero. Then the product of these two matrices would be a matrix with the only non-zero elements given by

$$(\boldsymbol{\alpha}_0^{\mathrm{SL}} (\mathbf{W}_0^{\mathrm{SL}})^{-1})_{n_{\mathrm{w}}+n_{\mathrm{b}},i} = x_i \quad (i = 1, \ldots, n_{\mathrm{w}} + n_{\mathrm{b}}) \tag{24}$$

In the same way, and taking into account that $\boldsymbol{\beta}_0^{\mathrm{SL}}$ given by (20) has only the extreme right element non-zero, we obtain as the only non-zero element

$$(\boldsymbol{\beta}_0^{\mathrm{SL}} (\mathbf{W}_0^{\mathrm{SL}})^{-1})_{1,j} = y_j \quad (j = 1, \ldots, n_{\mathrm{w}} + n_{\mathrm{b}}) \tag{25}$$

The particular values of x_i and y_j are not relevant for the discussion.

Then the matrix products involved in (21)–(23) would have as only non-zero elements

$$(\boldsymbol{\alpha}_0^{\mathrm{SL}}(\mathbf{W}_0^{\mathrm{SL}})^{-1}\boldsymbol{\beta}_0^{\mathrm{SL}})_{n_{\mathrm{w}}+n_{\mathrm{b}},n_{\mathrm{w}}+n_{\mathrm{b}}} = \boldsymbol{\alpha}_0^{\mathrm{bw}}(\mathbf{W}_0^{\mathrm{SL}})^{-1}_{1,1}\boldsymbol{\beta}_0^{\mathrm{wb}} \quad (26)$$

and

$$(\boldsymbol{\beta}_0^{\mathrm{SL}}(\mathbf{W}_0^{\mathrm{SL}})^{-1}\boldsymbol{\alpha}_0^{\mathrm{SL}})_{1,1} = \boldsymbol{\beta}_0^{\mathrm{wb}}(\mathbf{W}_0^{\mathrm{SL}})^{-1}_{n_{\mathrm{w}}+n_{\mathrm{b}},n_{\mathrm{w}}+n_{\mathrm{b}}}\boldsymbol{\alpha}_0^{\mathrm{bw}} \quad (27)$$

In this way (21) takes the form

$$\mathbf{W}_1^{\mathrm{SL}} = \begin{bmatrix} \mathbf{w}_0^{\mathrm{w}} - \boldsymbol{\beta}_0^{\mathrm{wb}}(\mathbf{W}_0^{\mathrm{SL}})^{-1}_{n_{\mathrm{w}}+n_{\mathrm{b}},n_{\mathrm{w}}+n_{\mathrm{b}}}\boldsymbol{\alpha}_0^{\mathrm{bw}} & \boldsymbol{\alpha}_0^{\mathrm{w}} & 0 & \cdots & \cdots & 0 \\ \boldsymbol{\beta}_0^{\mathrm{w}} & \mathbf{w}_0^{\mathrm{w}} & \boldsymbol{\alpha}_0^{\mathrm{w}} & 0 & \cdots & \vdots \\ 0 & \boldsymbol{\beta}_0^{\mathrm{w}} & \ddots & \ddots & 0 & \vdots \\ \vdots & 0 & \ddots & \cdots & \ddots & 0 \\ \vdots & \vdots & 0 & \ddots & \mathbf{w}_0^{\mathrm{b}} & \boldsymbol{\alpha}_0^{\mathrm{b}} \\ 0 & \cdots & \cdots & 0 & \boldsymbol{\beta}_0^{\mathrm{b}} & \mathbf{w}_0^{\mathrm{b}} - \boldsymbol{\alpha}_0^{\mathrm{bw}}(\mathbf{W}_0^{\mathrm{SL}})^{-1}_{1,1}\boldsymbol{\beta}_0^{\mathrm{wb}} \end{bmatrix} \quad (28)$$

In the same way (22) takes the form

$$\boldsymbol{\alpha}_1^{\mathrm{SL}} = \begin{bmatrix} 0 & 0 & \cdots & \cdots & \cdots & 0 \\ 0 & 0 & \cdots & \cdots & \cdots & \vdots \\ \vdots & \vdots & \vdots & \vdots & \vdots & \vdots \\ \vdots & \vdots & \vdots & \vdots & \vdots & \vdots \\ 0 & 0 & \cdots & \cdots & \cdots & \vdots \\ \boldsymbol{\alpha}_0^{\mathrm{bw}}(\mathbf{W}_0^{\mathrm{SL}})^{-1}_{1,n_{\mathrm{w}}+n_{\mathrm{b}}}\boldsymbol{\alpha}_0^{\mathrm{bw}} & 0 & \cdots & \cdots & \cdots & 0 \end{bmatrix} \quad (29)$$

and (23) takes the form

$$\boldsymbol{\beta}_1^{\mathrm{SL}} = \begin{bmatrix} 0 & 0 & \cdots & \cdots & 0 & \boldsymbol{\beta}_0^{\mathrm{wb}}(\mathbf{W}_0^{\mathrm{SL}})^{-1}_{n_{\mathrm{w}}+n_{\mathrm{b}},1}\boldsymbol{\beta}_0^{\mathrm{wb}} \\ 0 & 0 & \cdots & \cdots & \cdots & 0 \\ \vdots & \vdots & \vdots & \vdots & \vdots & \vdots \\ \vdots & \vdots & \vdots & \vdots & \vdots & \vdots \\ \vdots & \vdots & \vdots & \vdots & \vdots & \vdots \\ 0 & \cdots & \cdots & \cdots & \cdots & 0 \end{bmatrix} \quad (30)$$

From (28) it is clear that $\mathbf{W}_1^{\mathrm{SL}}$ keeps the tridiagonal block structure and only the $(1,1)$ and $(n_{\mathrm{w}}+n_{\mathrm{b}}, n_{\mathrm{w}}+n_{\mathrm{b}})$ elements are modified. $\boldsymbol{\alpha}_1^{\mathrm{SL}}$ and $\boldsymbol{\beta}_1^{\mathrm{SL}}$ keep the $\boldsymbol{\alpha}_0^{\mathrm{SL}}$ and $\boldsymbol{\beta}_0^{\mathrm{SL}}$ structure with only one non-zero element. It is then clear that successive iterations will not modify these structures. Then the iteration procedure is performed only on four blocks of size $(M \times M)$ in the different matrices involved. These blocks are obtained in a quick and accurate way by means of the method presented in [20], without the need of searching for the whole inverse matrix. After the convergence is reached we must invert the whole $\mathbf{W}^{\mathrm{SL}}$ matrix in order to obtain the superlattice Green function ($\mathbf{G}^{\mathrm{SL}} = (\mathbf{W}^{\mathrm{SL}})^{-1}$), thus inverting a big matrix only once. Thus using the structure of the matrices involved and the method for inverting block tridiagonal matrices of [20] we obtain an efficient computational method to obtain the superlattice Green function of discrete media.

We have obtained in a direct way all the Green function elements of the superlattice, as compared to the case of the structural Green function [11,19]. There we have to integrate over $\mathbf{k}_{\mathrm{SL}}$ in order to obtain the normal superlattice Green function, by using the interface projected Green function and additional relationships [11].

As a byproduct of the iteration procedure, and in the same way described in [17], we can obtain the following transfer matrices

$$\begin{aligned} \mathbf{G}_{N+1,N} &= \mathbf{T}_{\mathrm{SL}} G_{N,N} \\ \mathbf{G}_{N-1,N} &= \overline{\mathbf{T}}_{\mathrm{SL}} G_{N,N} \\ \mathbf{G}_{N,N+1} &= \mathbf{G}_{N,N} S_{\mathrm{SL}} \\ \mathbf{G}_{N,N-1} &= \mathbf{G}_{N,N} \overline{S}_{\mathrm{SL}} \end{aligned} \quad (31)$$

These transfer matrices can be used to study the properties of semiinfinite superlattices, multilayer systems formed with finite repetitions of the superlattice periods, etc., as explained in [11].

3. Results and discussion

In order to illustrate the capabilities of the new method we shall study the electronic structure of AlAs/GaAs superlattices. This is a well studied case and can serve as an excellent test system. We shall consider a realistic description by means of an ETB sp^3s^* Hamiltonian with nearest-neighbor interactions [15] and spin–orbit coupling [16]. The ETB parameters employed in our calculations are those given in [21]. We have employed the following energy reference: $E_v(\mathrm{AlAs}) = 0.00$ eV, $E_v(\mathrm{GaAs}) = 0.55$ eV.

As a preliminary test of the method we performed calculations for GaAs bulk systems. We considered "superlattices" ranging from 2 to 100 ML in the barrier and well. In the calculations the AlAs barrier was substituted by GaAs. The calculation time increased almost linearly with the period size. The results of our method were checked against those obtained by using the method described in [17]. The numerical values of the local density of states obtained by both methods agreed at least to 10^{-7}. Thus the electronic structure obtained by the two different methods is the same. This is a strong check on the numerical accuracy of our method.

It is a well known fact that different combinations of the (n_w, n_b) numbers of layers give rise to direct and indirect gap superlattices, and also to an intermediate region [10,22,23]. This can be a good test case for the new method. We have calculated then the lower conduction and higher valence band states for a wide number of AlAs/GaAs superlattices in order to illustrate this fact and to compare with recent experimental information [23]. In that work a transition from an indirect to a direct energy band structure was induced in short-period GaAs/AlAs superlattices by going from symmetric to asymmetric superlattices, and reducing the barrier thickness to half the well thickness.

We have seen in our calculations that for symmetric superlattices with $n_w \leqslant 8$ we have always indirect gap superlattices, that is type II superlattices.

In Table 1 we present the lowest electron state in the GaAs wells (E_0^Γ) and AlAs barriers (E_0^X) and compare them with those obtained by effective mass calculations [23]. It can be seen that for the symmetric superlattices (n_w, n_w) analyzed there the gap is indirect, except in our calculations for the (10,10) one. In those cases the lowest conduction band state is located at the X point in the AlAs barrier. By reducing the AlAs barrier width to the GaAs well half width the gap becomes direct. This can be seen in a graphic way in Fig. 1 where the local density of states (in arbitrary units) of the lowest conduction state is represented on the y-axis versus the position of the different anion and cation layers in the superlattice period. It can be seen how in the symmetric superlattices, Fig. 1(a) and Fig. 1(c), the lowest conduction state in the X point has the local density of states concentrated in

Table 1
Comparison of our results with those of [23]

Sample	n_w	n_w/n_b	E_0^Γ (eV)	E_0^X (eV)	$E_0^\Gamma - E_0^X m^*$	$E_0^\Gamma - E_0^X$ TB	Type
10/10	10	1	2.247	2.284	20	−37	I (II)
7/7	7	1	2.314	2.291	93	23	II
5/5	5	1	2.441	2.309	140	132	II
7/5	7	1.4	2.343	2.307	57	36	II
6/4	6	1.5	2.399	2.316	39	83	II
10/5	10	2	2.237	2.309	−47	−72	I
8/4	8	2	2.266	2.329	−34	−63	I
6/3	6	2	2.301	2.316	−31	−60	I

Well thickness in ML, ratio n_w/n_b of well to barrier thickness, ground conduction state energy of Γ state E_0^Γ in well and X state in barrier E_0^X, energy difference $E_0^\Gamma - E_0^X$ for our results and effective mass ones [20], and type of energy gap for investigated SLs.

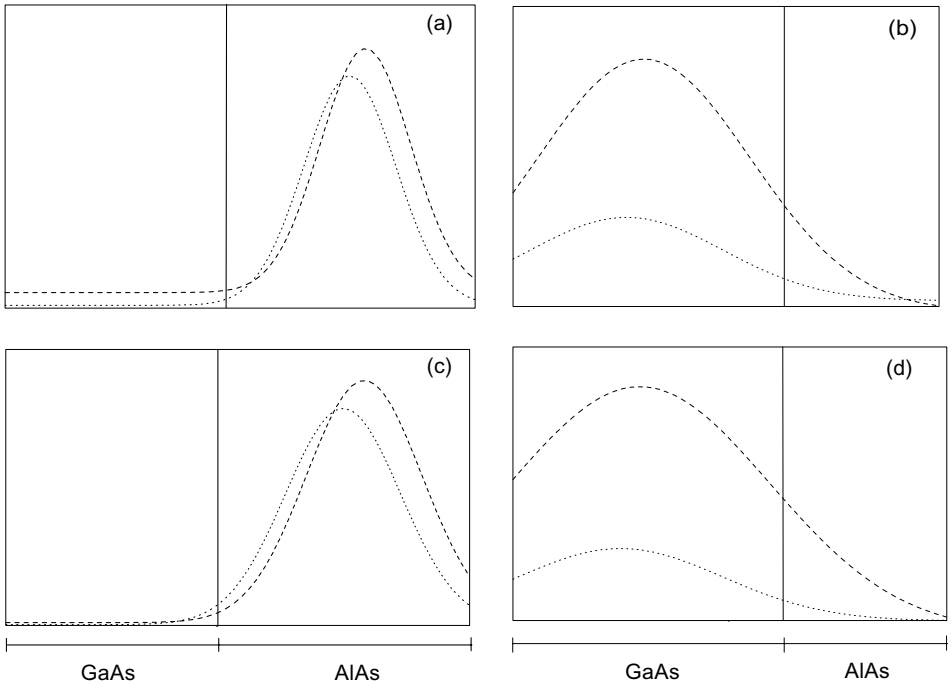

Fig. 1. Spatial distribution of the local density of states, in arbitrary units, versus the superlattice period, of the lowest conduction band state for (a) (8,8) (X point), (b) (8,4) (Γ point), (c) (6,6) (X point) and (d) (6,3) (Γ point) SLs. The figure displays the crossover of the X-state (symmetric SL) to the Γ state (antisymmetric SL). (Cations, dashed line; anions, dotted line.)

the AlAs layers. On the other hand in the asymmetric superlattices, Fig. 1(b) and (d), the lowest conduction state in the Γ point has the local density of states concentrated in the GaAs layers.

In Table 2 we present the results of our calculations for different superlattices grown experimentally [23], and studied by means of photoluminescence spectroscopy. The difference of the calculated and measured gaps is quite reasonable. The biggest differences appear for the (10,5) and (8,4) superlattices. It can be seen in [23] that those cases correspond to samples with 50 periods, whereas in the other cases the number of periods is at least 100, and there can be some further differences added to the non-inclusion in our calculations of exciton effects. Our results give also

Table 2
Comparison of our results with those of [23]

Sample	n_w	n_w/n_b	E_c	E_v	$(E_c - E_v)_{TB}$	$(E_c - E_v)_{Exp}$	$\Delta E_{Exp} - \Delta E_{Theor}$	Type
10/10	10	1	2.247	0.483	1.764	1.804	0.040	I (II)
7/7	7	1	2.291	0.440	1.851	1.866	0.015	II
5/5	5	1	2.309	0.390	1.919	1.939	0.020	II
7/5	7	1.4	2.307	0.443	1.864			II
6/4	6	1.5	2.316	0.425	1.891			II
10/5	10	2	2.237	0.484	1.753	1.846	0.093	I
8/4	8	2	2.266	0.463	1.803	1.902	0.099	I
6/3	6	2	2.301	0.433	1.868	1.921	0.053	I

Well thickness in ML, ratio n_w/n_b of well to barrier thickness, ground state energy in conduction (E_c) and valence (E_v) band, energy difference $E_c - E_v$ for our results, energy difference $E_c - E_v$ for experimental ones, the discrepancy $\Delta E_{Exp} - \Delta E_{Theor}$ of our results respect to experimental data [23] (the energy units are eV) and type of energy gap for investigated SLs.

similar results to those of [10], with some small differences due to the different parametrization.

From the computational point of view the new algorithm is fast, with very good precision and convergence, as checked against [17] in the bulk case. Besides this the new algorithm allows us to consider large period SL, without any computational problem. This algorithm is not restricted to rectangular potential profiles, and any form can be considered, at least in principle. Thus the scope of our method is wider and allows us to consider problems such as parabolic SLs, Stark effect in SLs, to mention some ones.

Thus it has been shown that this new method provides an efficient way to calculate electronic, vibrational, etc., properties of superlattices.

4. Conclusions

We have developed a new method to calculate the Green function of discrete superlattices. The basic idea is to consider the whole superlattice period in order to obtain the corresponding transfer matrices, and the superlattice Green function. This is done by the generalization of the classical algorithm for the transfer matrix [17] together with a method for the inversion of block tridiagonal matrices [20]. The method is an efficient and reliable one. It has been checked by studying the electronic properties of AlAs/GaAs superlattices described by means of a realistic sp^3s^* ETB Hamiltonian. Comparison of our results against experimental data and other theoretical methods gives a very good agreement.

Acknowledgements

This work has been partially supported by the Ministerio de Ciencia y Tecnología (Spain) through Grant MAT2003-04278, and by CONACyT (México) through Grant-J44741-F.

References

[1] B. Vinter, C. Weisbuch, Quantum Semiconductor Structures, Academic Press, San Diego, 1991.
[2] St. Giugni, T.I. Tansley, G.J. Griffiths, J. Cryst. Growth 111 (1991) 50.
[3] F. Capasso, H.M. Cox, A.L. Hutchinson, N.A. Olsson, S.G. Hummel, Appl. Phys. Lett. 45 (1984) 1193.
[4] G. Ihm, S.K. Noh, J.H. Lee, J.-S. Hwang, T.W. Kim,, Superlatt. Microstruct. 12 (1995) 155.
[5] R. Merlin, K. Bajema, R. Clarke, F.-Y. Juang, P.K. Bhattacharya, Phys. Rev. Lett. 55 (1985) 1768.
[6] A.A. Yamaguchi, T. Saiki, T. Tada, T. Minomiya, K. Misawa, T. Kobayashi, M. Kuwata-Gonokami, T. Yao, Solid State Commun. 75 (1990) 955.
[7] G. Strasser, S. Gianordoli, L. Hvozdara, W. Schrenk, K. Unterrainer, E. Gomik, Appl. Phys. Lett. 75 (1999) 1345.
[8] A. di Carlo, Phys. Stat. Sol. (b) 217 (2000) 703.
[9] A. di Carlo, Semicond. Sci. Technol. 18 (2003) R1.
[10] M.C. Muñoz, V.R. Velasco, F. Garcia-Moliner, Phys. Rev. B 39 (1989) 1786.
[11] F. García-Moliner, V.R. Velasco, Theory of Single and Multiple Interfaces, Word Scientific, Singapore, 1992.
[12] L. Fernández-Alvarez, G. Monsivais, S. Vlaev, V.R. Velasco, Surf. Sci. 369 (1996) 367.
[13] L. Dobrzynski, Surf. Sci. 175 (1986) 1.
[14] L. Dobrzynski, Surf. Sci. Rep. 6 (1986) 119.
[15] P. Vogl, H.P. Hjalmarson, J.D. Dow, J. Phys. Chem. Solids 44 (1983) 365.
[16] D.J. Chadi, Phys. Rev. B 16 (1977) 790.
[17] M.P. López Sancho, J.M. López-Sancho, J. Rubio, J. Phys. F 14 (1984) 1205;
M.P. López Sancho, J.M. López-Sancho, J. Rubio, J. Phys. F 15 (1985) 851.
[18] D.H. Lee, J.D. Joannopoulos, Phys. Rev. B 23 (1981) 4988.
[19] J. Arriaga, F. Garcia-Moliner, V.R. Velasco, Prog. Surf. Sci. 42 (1993) 271.
[20] S. Vlaev, V.R. Velasco, F. Garcia-Moliner, Phys. Rev. B 49 (1994) 11222.
[21] D.A. Contreras-Solorio, V.R. Velasco, F. García-Moliner, Phys. Rev. B 47 (1993) 4651.
[22] J. Ihm, Appl. Phys. Lett. 50 (1987) 1068.
[23] S. Krylyuk, D.V. Korbutyak, V.G. Litovchenko, R. Hey, H.T. Grahn, K.H. Ploog, Appl. Phys. Lett. 74 (1999) 2596.